



# The strain rate and temperature effects on the static and dynamic properties of S2 glass/epoxy composites

Zafer Kaya<sup>1</sup> · Hüseyin Ersen Balcioglu<sup>2</sup> · Halit Gün<sup>2</sup>

Received: 7 January 2020 / Accepted: 26 July 2020 / Published online: 4 August 2020  
© Springer-Verlag GmbH Germany, part of Springer Nature 2020

## Abstract

The environmental conditions, the loads during service, the resistance of the materials against these loads and also the price/benefit ratios affect the choice of materials. S2 glass-reinforced polymer composites are among the most widely used composite structures, especially when high strength and low cost are required. Polymer matrix composite materials show ductile damage at high temperatures and brittle damage mechanism at low temperatures. Therefore, environmental temperature is a parameter that restricts the use of polymer matrix composites. In this study, mechanical characterization of S2 glass/epoxy-laminated composites was investigated at different environment temperature ( $-20\text{ }^{\circ}\text{C}$ ,  $0\text{ }^{\circ}\text{C}$ ,  $20\text{ }^{\circ}\text{C}$ , and  $80\text{ }^{\circ}\text{C}$ ) and different strain rate ( $8.3 \times 10^{-3}$ ,  $8.3 \times 10^{-4}$ , and  $8.3 \times 10^{-5}\text{ s}^{-1}$ ). In this context, quasi-static tensile, and compressive tests were performed. In addition, S2 glass/epoxy composites were subjected to dynamic mechanical analysis (DMA) under variable temperature and load to examine their viscoelastic behavior. Another test to better characterize the composite structure of the S2 glass/epoxy material was thermogravimetric analysis (TGA). Test results showed that the S2 glass/epoxy composite structure is sensitive to the variable deformation rate and variable ambient temperature.

**Keywords** S2 glass/epoxy · Strain rate effect · Temperature effect · Mechanical properties · Dynamical mechanical analysis (DMA) · TGA analysis

## 1 Introduction

The usage of high-performance fiber for structural applications that require high strength is increasing day by day. In this context, synthetic fiber types such as carbon, aramide, dyneema and glass fiber are the most frequently used. Glass fiber has been widely used in the manufacturing of polymer-based composite materials. Glass fibers have comparable mechanical properties to other synthetic fibers such as carbon and aramide fiber [1]. In addition, the mechanical and electrical properties of the composite material can be enhanced by reinforcing the nanoparticles into the glass fibers. In this respect, glass fiber is a type of fiber that is also suitable for nanocomposite applications [2–4]. Among glass fiber types, E-glass is the most commonly used type. However, when

the strength and stiffness of the E-glass are not sufficient, S2-glass fiber that is higher durable than E glass is used. S2 glass fiber-reinforced polymer composites have ultimate properties such as corrosion resistant, fatigue, and impact strength when compared with traditional glass fiber. Modern developments in land, sea, and air transport industries have increased the use of these materials. As the S2 glass fiber-reinforced composite structures are increasingly used in these industries, there are many studies investigating the mechanical characterization of this type of composite structure [5–11].

Fiber-reinforced polymer matrix composite structures (FRP) are sensitive to environmental influences. Excessive environmental conditions, such as warm, humid, and freezing can exacerbate the mechanical strength of FRP composites. In addition, the loads that are applied during the service life on the composite structure cause the development of the typical damage mechanisms such as matrix cracks, fiber breakage, fiber–matrix separation (delamination) for polymer matrix composites. Physical and mechanical behavior of a thermosetting matrix depends on temperature. When the temperature approaches the glass transition temperature

✉ Hüseyin Ersen Balcioglu  
ersen.balcioglu@usak.edu.tr

<sup>1</sup> Graduate School of Natural and Applied Sciences, Usak University, Uşak, Turkey

<sup>2</sup> Department of Mechanical Engineering, Usak University, Uşak, Turkey

of the polymer, the strength of matrix reduces dramatically. There are a limited number of studies examining the effects of environmental effects on the physical and mechanical properties of polymer composites. Moudood et al. [12] have investigated the environmental effects such as water immersion, warm humid environment, and freeze–thaw conditions on the durability and the mechanical performance of polymer composites. Yang et al. [13] have studied the effects of a cold environment on the mechanical and impact behavior of natural cotton-reinforced epoxy composites. Hulugappa et al. [14] have conducted a study on flexural and fracture toughness of hybrid polymer composites at room temperature, elevated temperature and cryogenic temperature. They observed that fracture toughness of polymer composites improved about 26% at cryogenic temperature and decreased 12.5% at elevated temperature. Scida et al. [15] found that the tensile properties of the flax composites are influenced by hydrothermal aging. At 90% RH and 20 °C, the reduction of Young's modulus was 33% for the first 3 days and reduced by 55% after 38 days. Nikolaev et al. [16] have investigated the effect of constant and cyclic temperature influences from – 196 to 120 °C on composite materials. Aklilu et al. [17] have conducted an experimental study on the short beam shear and dynamic mechanical analysis tests for the composite specimens, which are exposed to temperatures ranging from 25 to 140 °C. The results indicate that the interlaminar shear failure strength and stiffness of polymer composite degrade with increasing temperature.

To develop physical-based constitutive models based on micro-mechanics or laminate theory, it is important to understand the strain rate effects not only on the polymer composite but also on the individual constituents, i.e., the fiber and the matrix. As expected with a polymeric matrix, the bigger the strain rate, the bigger the elastic modulus and the tensile strength, and the lower the maximum strain [18]. In the literature, there are studies investigating the mechanical behavior of laminated composites under different strain rates. Staab and Gilat [19] have studied strain rate effects on the mechanical behavior of glass/epoxy angle-ply laminates. Results indicated that the maximum normal stress experienced by glass/epoxy is higher for dynamic than quasi-static loading conditions. Aktas et al. [20] investigated the tensile and compressive behavior of woven-knitting glass/epoxy composites under a low strain rate. Chen et al. [21] have performed uniaxial tensile tests, in which strain rate varies in the range between  $10^{-3}$  and  $10^3$  s<sup>-1</sup>, for short glass and carbon fiber-reinforced PEEK composites. Okoli and Smith [22] have examined tensile tests at different strain rates on the glass/epoxy composites to determine the effects of strain rate on the Poisson's ratio of the composite material. Test results showed that the Poisson ratio is not sensitive to the tensile speed but to the state of the fibers in the composites. Saniee et al. [23] have investigated the strain rate effects on

the tensile behavior of glass/epoxy composites at low strain rates.

Polymers respond to the energy of motion in two ways: (1) elastic response which is important for shape recovery and (2) viscous response which is essential for dispersing mechanical energy and preventing breakage. Dynamic mechanical analysis (DMA) is an important technique used to measure the mechanical and viscoelastic properties of materials such as thermoplastics, thermosets, elastomers, ceramics, and metals. In the DMA, the sample is periodically stressed in one of the several deformation modes (bending, pulling, shearing and compression) [24]. Vasudevan et al. [25] have characterized the viscoelastic behavior of glass and carbon fiber-reinforced composite using dynamic mechanical analyzer over the temperature range of 30–150 °C at four different frequencies such as 1, 10, 50 and 100 Hz. Haque and Shamsuzzoha [26] investigated the mechanical and thermal properties of nano clay filled S2-glass/epoxy nanocomposites using thermo gravimetric Analysis (TGA) and Dynamic Modulus Analyzer. Rangaraj et al. [27] have employed the DMA technique to determine the temperature effect on the storage and loss moduli for Kevlar–glass/epoxy hybrid composites.

In the present study, the mechanical properties of S2 glass/epoxy-reinforced composites were investigated under different strain rates and different temperatures. Also, dynamic mechanical analysis (DMA) tests were performed at different temperature ranges (– 30 °C and 200 °C) to determine the viscoelastic behavior of S2 glass/epoxy composites. In addition to these mechanical investigations, TGA analysis was performed to better define the relationship between resin/hardener set and S glass fiber fabric.

## 2 Materials and methods

### 2.1 Manufacturing of laminated composite

Materials used in the present study are epoxy resin (Hexion MGS L285) with hardener (Hexion H287) and woven fabric of S2 glass, which manufactured with weight 190 g/m<sup>2</sup> and thickness 130 µm. Epoxy resin was prepared by mixing resin and hardener in ratios of 60:40, respectively. The elastic properties of used S2 glass fiber and epoxy resin are given in Table 1 [28, 29].

The dry S2-glass woven preforms were cut into plies with a 500 × 400 mm dimension and stacked in eight layers on an open mold with a peeling cloth in between the fabric and the mold. A separate peeling cloth and distribution mesh were placed over the preform followed by a vacuum plastic bag. The laminated composite having eight layers was produced using the Vacuum-Assisted Resin Transfer Molding (VARTM) method. While manufacturing with the

**Table 1** The material properties of fiber material and epoxy resin

Material properties	Fiber material (S2-glass)[28]	Matrix material (hexion epoxy resin) [29]
Young's modulus ( $E$ ) in GPa	86–93	3.2
Shear modulus ( $G$ ) in GPa	35–39	1.18
Poisson's ratio ( $\nu$ )	0.21	0.36
Tensile strength in MPa	4700–4800	70–80
Compressive strength in MPa	4000–5000	120–140

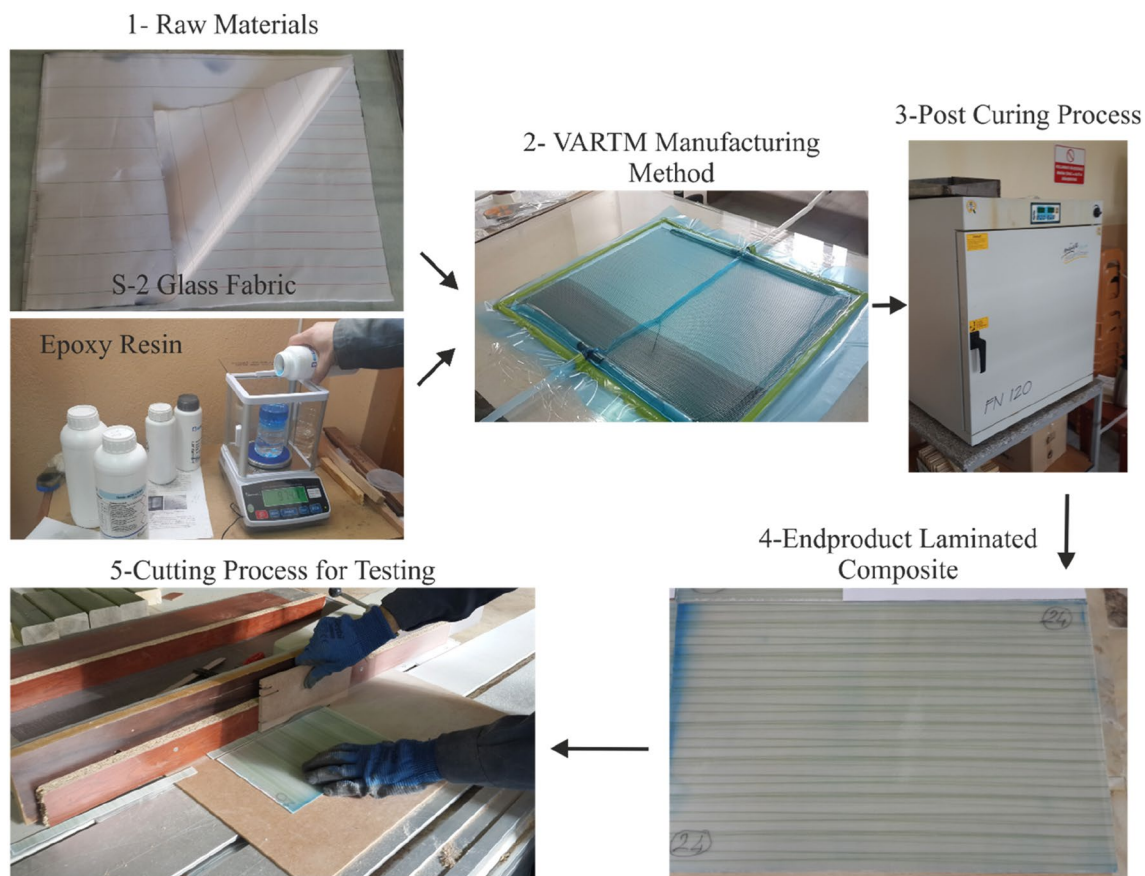
VARTM method, epoxy resin was saturated on S2 glass fabric material under a vacuum value of approximately 650 mmHg. After S2 glass fabrics were completely saturated by the matrix material, the process was stopped and the wetted plies were left for curing under vacuum at room temperature for 24 h. The post-curing was done in an drying oven at 80 °C for 5 h. The internal environment of the drying oven has atmospheric pressure and dry air environment. The flow chart for the production of S2 glass fiber-reinforced laminated composite plates is illustrated in Fig. 1.

## 2.2 Determination of mechanical properties

To investigate the effects of strain rates and temperature on the mechanical behavior of S2 glass/epoxy composites, tensile, compression, and shear test was performed. These mechanical tests were carried out at  $-20$  °C,  $0$  °C,  $20$  °C and  $80$  °C ambient temperature conditions and  $0.5$  mm/min,  $5$  mm/min and  $50$  mm/min tester cross-head velocity. Tensile and compression tests were carried out on a Shimadzu AG-X model 100 kN capacity temperature-controlled test device with the thermostatic chamber (Fig. 2a).

The tensile tests were carried out according to ASTM D3039 test standard [30]. Tensile test specimens having dimension  $15 \times 200$  mm in warp direction and  $25 \times 200$  mm in weft direction were cut [5, 22, 31]. The elasticity modulus in the warp direction ( $E_1$ ), a tensile strength in the warp direction ( $T_1$ ), the elasticity modulus in the weft direction ( $E_2$ ), and tensile strength in the weft direction ( $T_2$ ) were found depending on the fiber orientation. A bi-axial video extensometer was used to measure the elongation of the test specimen (Fig. 2b).

ASTM D 3410 test standard was employed to perform the compressive test. This test method determines the in-plane

**Fig. 1** Manufacturing flowchart of S2 glass/epoxy-laminated composites



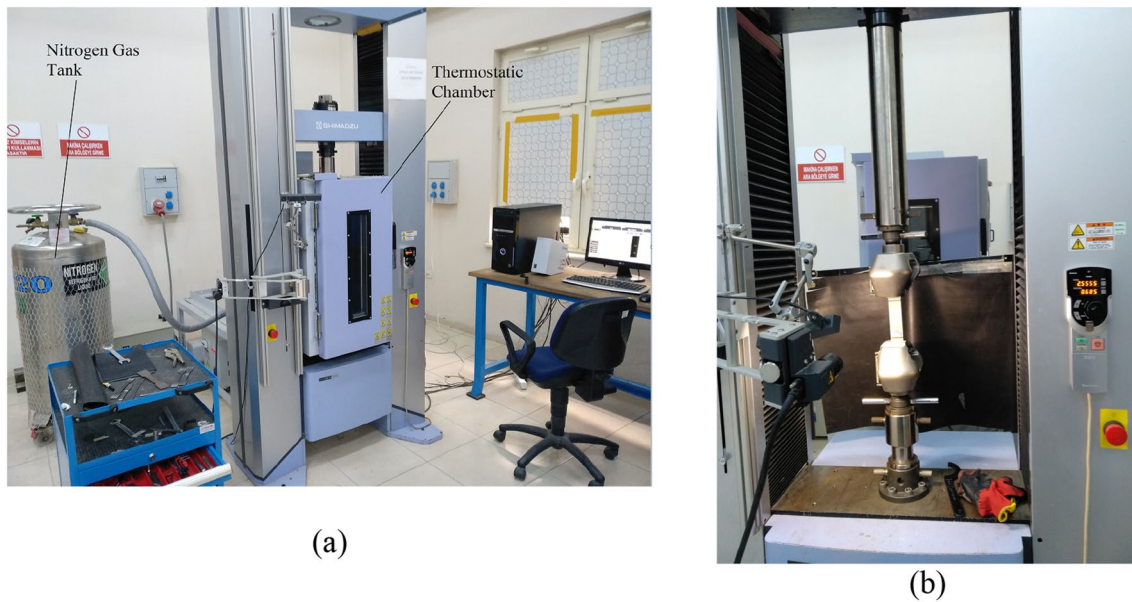


**Fig. 2** **a** Shimadzu AG-X universal test device, and **b** bi-axial video extensometer

compressive properties of polymer matrix composite materials reinforced by high modulus fiber [32].  $10 \times 140$  mm dimensions in the warp direction and  $25 \times 140$  mm dimensions in weft direction were cut and compression tests were carried out. IITR test method was used to determine compression stress (Fig. 3).

The warp direction compression stress ( $C_1$ ) and the weft direction compression stress ( $C_2$ ) were determined by dividing the damage load by the sample cross-sectional area. Five samples were tested for each property of S2 glass/epoxy composites at the same strain rate and temperature.

### 2.3 Dynamic mechanical analysis (DMA)

Dynamic mechanical analysis (DMA) is the most useful technique to characterize the viscoelastic behavior of polymers materials. Furthermore, this test method can be

used to find the glass transition temperature of the material being tested. Polymer viscoelasticity is dependent on temperature and time. Controlled heating and cooling are incorporated in DMA instruments to study the temperature effects on polymer stiffness and resiliency. This test was carried out according to ASTM D7028 standard with S2 glass/epoxy composite warp direction, weft direction and diagonal ( $45^\circ$  fiber direction) with three fiber direction test specimens. This test method covers the procedure for the determination of the dry or wet glass transition temperature ( $T_g$ ) of polymer matrix composites [33]. Dimensions of DMA specimens are  $53 \times 11.5 \times 1.75$  mm in length, width, and thickness, respectively (Fig. 4). The tests were carried out in the 3-point bending test type at a frequency of 1 Hz, increase  $5^\circ\text{C}/\text{min}$  and between the temperature of  $-30^\circ\text{C}$  and  $200^\circ\text{C}$ .



**Fig. 3** Compression test specimens, standard clamping apparatus

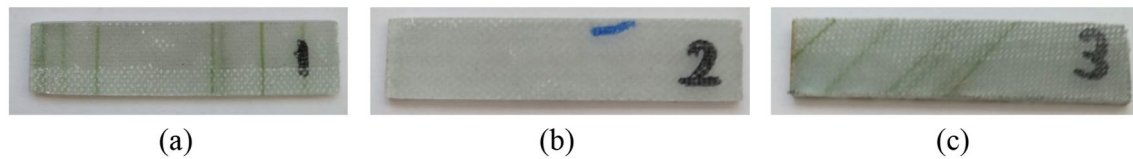


Fig. 4 DMA specimens, a warp, b weft and c diagonal direction

### 2.4 Thermogravimetric analysis (TGA)

Thermogravimetric analysis (TGA) is a technique in which the mass of the test sample is monitored in a controlled atmosphere and under a controlled temperature program as a function of temperature or time. The resin content, and by extension the fiber volume, of S2 glass fiber/epoxy composite laminates, were measured using thermogravimetric analysis (TGA) in a nitrogen atmosphere. The tests were performed on the basis of the ASTM E 1131-08 standard. This test method provides a general technique incorporating thermogravimetric to determine the amount of highly volatile matter, medium volatile matter, combustible material, and ash content of compounds [34]. The test specimens were tested by increasing the temperature of 10 °C/min between 25 and 600 °C. Experiments were performed on the Hitachi STA 7300 TGA test device.

## 3 Results and discussion

### 3.1 Static tests

Static tests were performed in two stages as tensile and compression tests. The tensile and compressive test were carried out at the cold, room and high temperature (− 20 °C, 0 °C, 20 °C, and 80 °C) at three cross-head velocities (0.5, 5

and 50 mm/min). These velocities correspond to  $8.3 \times 10^{-5}$ ,  $8.3 \times 10^{-4}$ , and  $8.3 \times 10^{-3} \text{ s}^{-1}$  strain rate, respectively. The tensile test results show that the load-bearing capacity and deformation ability of the composite structure is directly related to the strain rate. Figure 5 shows the tensile load and displacement curves of the composite material at different strain rates depending on the time for the coldest and warmest environment in the warp direction. No graph was given in weft direction since weft fiber direction shows similar behavior to warp direction. Accordingly, when the strain rate increases, there is not much change in the load-carrying capacity of the composite sample, but there is a noticeable change in the deformation ability.

Figure 6 shows the tensile stress–strain curves of S2 glass/epoxy composites under various temperatures and strain rates in the warp direction. Stress–strain behaviors obtained from maximum and minimum values of the examined parameters were given to obtain the simple and understandable graphs.

As seen in Fig. 5, if the strain rate increases, the stress and strain values increase in a linear form for the same temperature value. In spite of that, it cannot be said to have a linear effect on the stress and strain values for increasing in temperature at the same strain rate. The maximum tensile stress and tensile strain, which correspond to tensile damage load ( $P_T$ ), were given in Tables 2 and 3 for each examined temperature and strain rate values in warp and weft direction, respectively. The

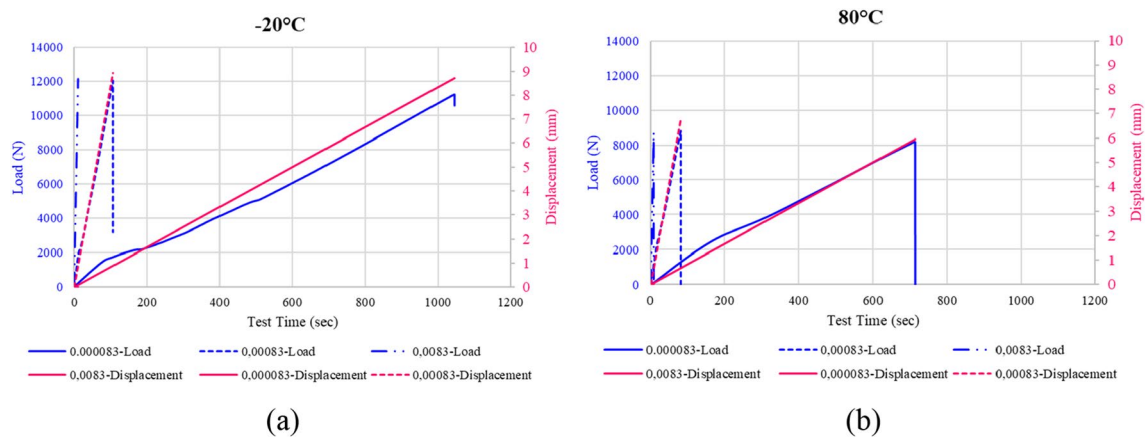
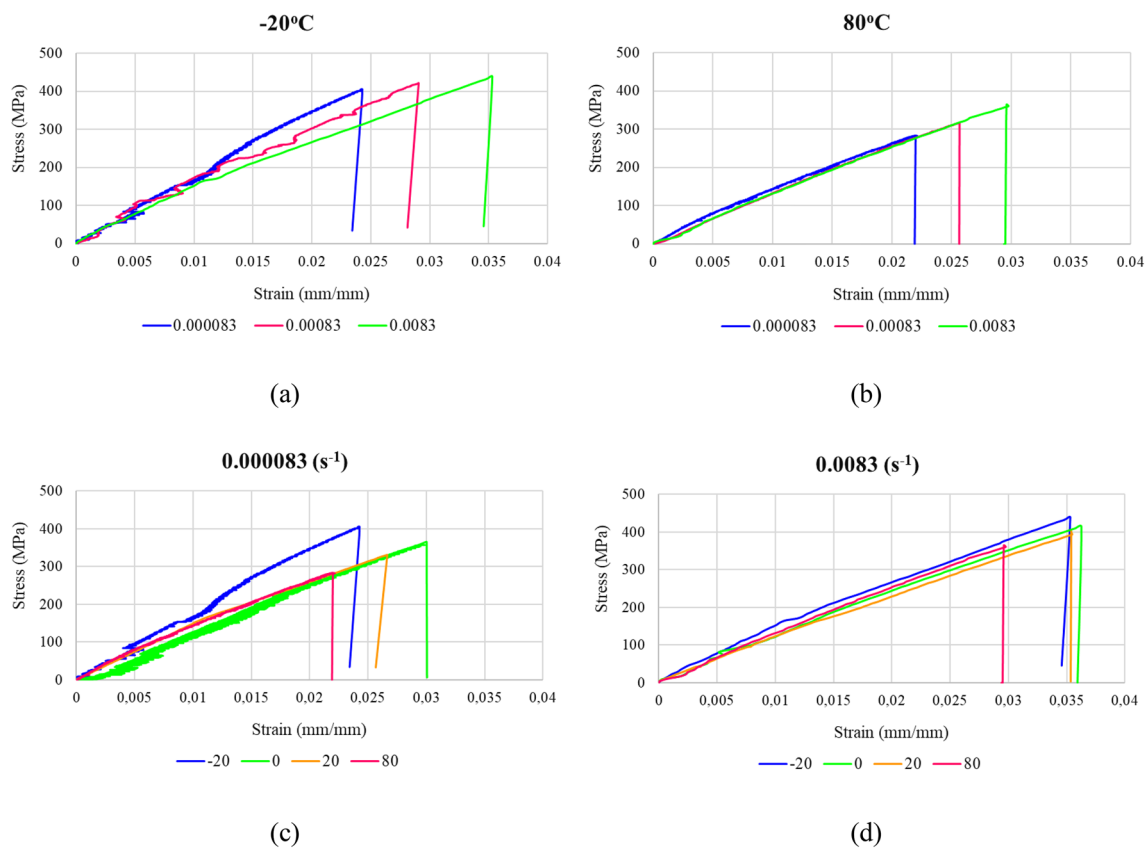


Fig. 5 The load–displacement and time relationship obtained from the tensile test a – 20 °C and b 80 °C



**Fig. 6** The tensile stress–strain curves of S2 glass/epoxy composites under various temperature (**a** – 20 °C and **b** 80 °C) and strain rates (**c** 0.000083 s<sup>-1</sup> and **d** 0.0083 s<sup>-1</sup>) in warp direction

**Table 2** The maximum tensile stress ( $T_1$ ) and strain values corresponding to this stress in warp direction

Strain rates (/s <sup>-1</sup> )	– 20 °C		0 °C		20 °C		80 °C	
	Stress (MPa)	Strain (mm/mm)	Stress (MPa)	Strain (mm/mm)	Stress (MPa)	Strain (mm/mm)	Stress (MPa)	Strain (mm/mm)
0.000083	403.31	0.0242	356.45	0.0304	330.98	0.0260	280.80	0.0223
0.00083	421.75	0.0290	419.65	0.0347	364.64	0.0326	318.13	0.0256
0.0083	438.68	0.0353	421.35	0.0362	393.41	0.0354	360.72	0.0297

**Table 3** The maximum tensile stress ( $T_2$ ) and strain values corresponding to this stress in weft direction

Strain rates (/s <sup>-1</sup> )	– 20 °C		0 °C		20 °C		80 °C	
	Stress (MPa)	Strain (mm/mm)	Stress (MPa)	Strain (mm/mm)	Stress (MPa)	Strain (mm/mm)	Stress (MPa)	Strain (mm/mm)
0.000083	329.15	0.0162	323.26	0.0178	298.09	0.0195	252.94	0.0178
0.00083	341.39	0.0171	341.36	0.0197	336.92	0.0217	275.69	0.0199
0.0083	381.19	0.0179	354.79	0.0215	345.49	0.0237	284.33	0.0219

maximum tensile stress and the maximum tensile strain were calculated according to Eqs. (1–2), respectively:

$$T_{\text{Stress}} = \frac{P_T}{A}, \tag{1}$$

$$T_{\text{Strain}} = \frac{L_T}{L_{T\text{-Gage}}}, \tag{2}$$

where  $P_T$  and  $L_T$  are the tensile damage load and displacement value at the time the test sample is damaged,

respectively.  $A$  is the load-bearing cross-sectional area of the test sample.  $L_{T-Gage}$  is the length of the tensile test sample between the gripping jaws.

The maximum tensile strength of S2 glass/epoxy composite in the warp and weft direction was found to be 438.68 MPa and 381.19 MPa, respectively at a cross-head velocity of 50 mm/min at  $-20\text{ }^\circ\text{C}$  ambient temperature. Similarly, the minimum tensile strength in the warp and weft direction was 280.80 MPa and 252.94 MPa, respectively, at a cross-head velocity of 0.5 mm/min at  $80\text{ }^\circ\text{C}$  ambient temperature. Maximum tensile strength decreased with increasing temperature in test specimens both in the warp direction and weft direction. Also, tensile strength showed an upward trend with an increase in the tensile speed. Generally, the ambient conditions of production and use of polymer composites are room temperature ( $20\text{ }^\circ\text{C}$ ). Thus, if the stress and strain values at  $20\text{ }^\circ\text{C}$  were referenced, it was seen that there was a maximum 22% increase in the tensile stress of S2 glass/epoxy; on the other hand, there was a maximum 24% decrease in the tensile strain for the cold environment ( $-20\text{ }^\circ\text{C}$ ) at same strain rate value. If a similar comparison is made for high temperature ( $80\text{ }^\circ\text{C}$ ), it is observed that there is a maximum decrease of 18% in tensile stress and a maximum decrease of 21% in tensile strain.

The other mechanical properties obtained from the static tensile test are the modulus of elasticity in the warp ( $E_1$ ) and weft ( $E_2$ ) direction of the S2 glass/epoxy. The elasticity module is a measure of the resistance of the composite material to elastic deformation.

This value was calculated according to Eq. (3) with the help of Hooke's Law from the elastic region of the stress-strain curve (Fig. 6):

$$E = \frac{\sigma_a - \sigma_b}{\epsilon_a - \epsilon_b}, \tag{3}$$

$\sigma$  and  $\epsilon$  are the stress and strain values at any point  $a$  and  $b$ , located in the elastic region of the stress-strain curve, respectively. The elasticity modulus values, which depended on the fiber direction, are given in Table 4 for different temperatures and strain rates. When the tensile tests on the warp and weft direction of S2 glass/epoxy composite are examined, the highest elastic modulus according to the woven directions was seen as 18.74 GPa and 21.19 GPa, respectively. These moduli of elasticity were formed at a tensile

speed of 50 mm/min at  $-20\text{ }^\circ\text{C}$ . The lowest elasticity modulus in warp and weft direction was observed at a temperature of  $80\text{ }^\circ\text{C}$  and tensile speed of 0.5 mm/min as 16.18 GPa and 15.41 GPa, respectively. When the elasticity modulus at the same temperature and strain rate is compared according to fiber directions, it is seen that the elasticity modulus in the weft direction is higher up to 13% than the wrap direction. If the modulus of elasticity at  $20\text{ }^\circ\text{C}$  is taken as a reference, it is observed that there is a maximum increase of 9% in the wrap direction elasticity modulus for the cold environment and a maximum decrease of 4% for the warm environment. When a similar comparison was made for weft direction, a maximum 12% increase was seen in the coldest environment for the modulus of elasticity and an 11% decrease for the warmest environment.

The load-displacement-time relationship obtained from the specimens subjected to compression testing with respect to the warp fiber direction is shown in Fig. 7.

Also, Fig. 8 expressed the effect of temperature and strain rate on stress-strain behavior for the compression load. For the compression behavior of S2 glass/epoxy composite, although there is a linear relationship between the strain rate increasing and the stress-strain values, the same linear relationship cannot be mentioned when the temperature increases from  $-20$  to  $80\text{ }^\circ\text{C}$ .

The maximum compression stress and the maximum compression strain were calculated according to Eqs. (4-5), respectively:

$$C_{Stress} = \frac{P_C}{A} \tag{4}$$

$$C_{Strain} = \frac{L_C}{L_{C-Gage}}, \tag{5}$$

where  $P_C$  and  $L_C$  are the compression damage load and displacement value at the time the test sample is damaged, respectively.  $A$  is the load-bearing cross-sectional area of the test sample.  $L_{C-Gage}$  is the length of the tensile test sample between the gripping jaws.

The maximum compression stress and compression strain, which correspond to compression damage load, are given in Tables 5 and 6 for each examined temperature and strain rate values in warp and weft direction, respectively. When the stress and strain values obtained at room temperature ( $20\text{ }^\circ\text{C}$ )

**Table 4** Elasticity modulus of S2 glass/epoxy in the warp ( $E_1$ ) and weft ( $E_2$ ) direction

Strain rate ( $/s^{-1}$ )	$E_1$ (GPa)				$E_2$ (GPa)			
	$-20\text{ }^\circ\text{C}$	$0\text{ }^\circ\text{C}$	$20\text{ }^\circ\text{C}$	$80\text{ }^\circ\text{C}$	$-20\text{ }^\circ\text{C}$	$0\text{ }^\circ\text{C}$	$20\text{ }^\circ\text{C}$	$80\text{ }^\circ\text{C}$
0.000083	18.59	18.32	16.85	16.18	19.53	18.13	17.19	15.41
0.00083	18.61	18.39	16.92	16.29	19.68	18.25	17.39	15.66
0.0083	18.74	18.50	17.00	16.34	21.19	18.88	17.92	17.24

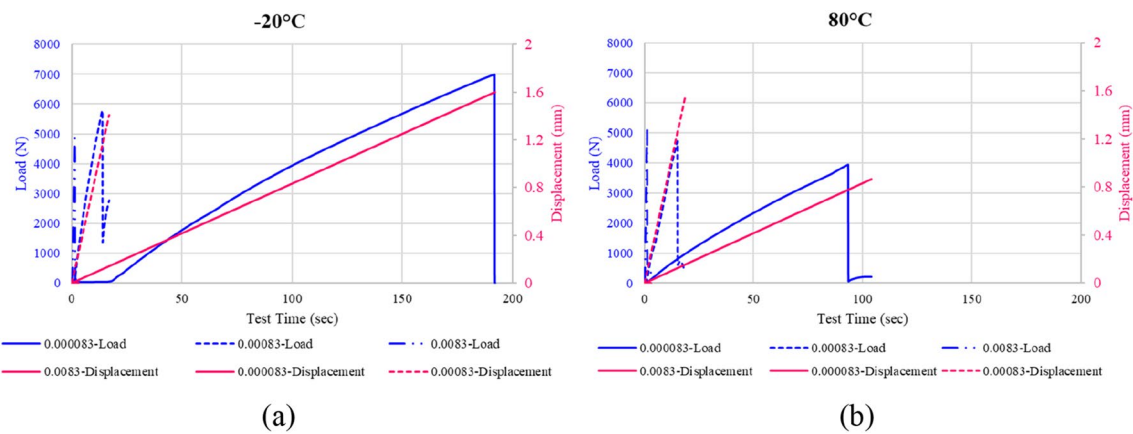


**Fig. 7** The load–displacement and time relationship obtained from compression test **a** – 20 °C and **b** 80 °C

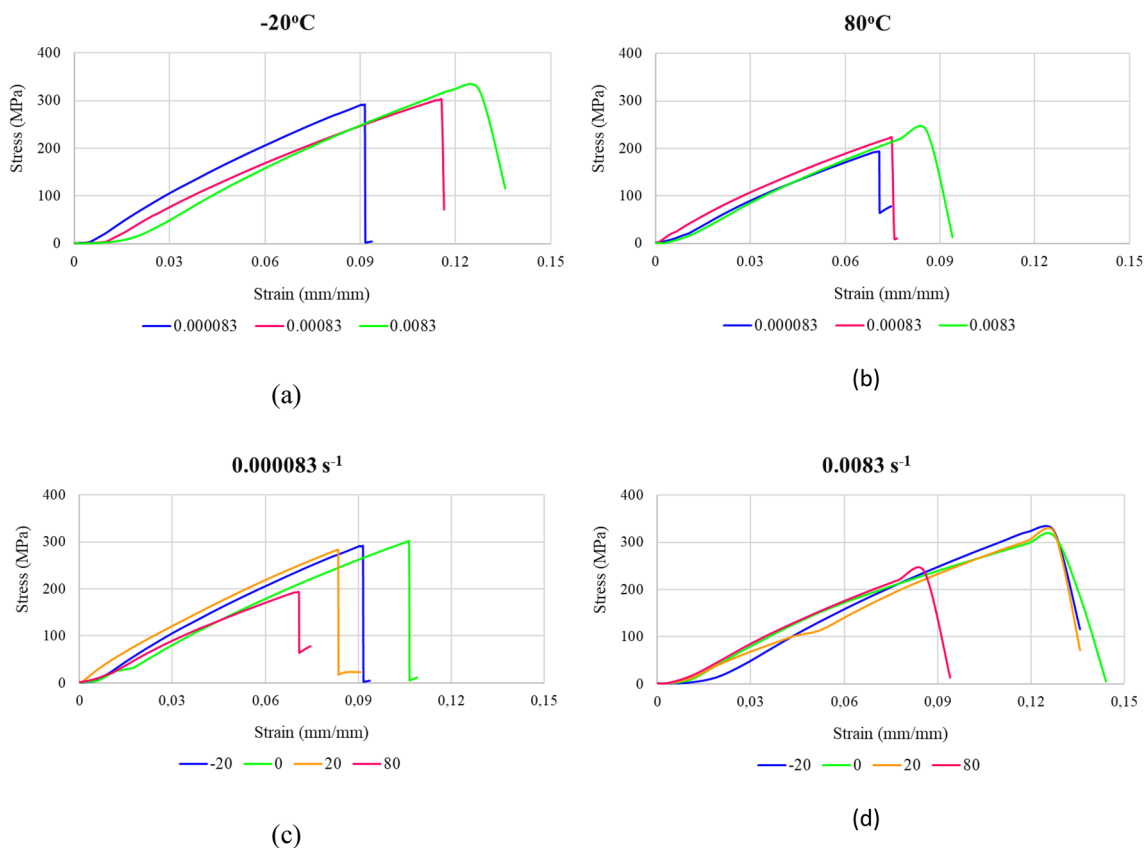


**Fig. 8** The compression stress–strain curves of S2 glass/epoxy composites under various temperature (**a** – 20 °C and **b** 80 °C) and strain rates (**c** 0.000083 s<sup>-1</sup> and **d** 0.0083 s<sup>-1</sup>) in warp direction

under compressive load were taken as reference, a maximum increase of 16% in compression stress and a maximum increase of 51% in compression strain was observed for the cold environment (– 20 °C). When the stress–strain values obtained at high temperature (80 °C) were compared with

its room temperature (20 °C), a maximum 30% decrease in compression stress value and a maximum 32% decrease in compression strain value were observed.

The absorbed fracture energy values for both tensile and compression tests are summarized in Tables 7 and



**Table 5** The maximum compression stress ( $C_1$ ) and strain values corresponding to this stress in warp direction

Strain rates ( $/s^{-1}$ )	− 20 °C		0 °C		20 °C		80 °C	
	Stress (MPa)	Strain (mm/mm)	Stress (MPa)	Strain (mm/mm)	Stress (MPa)	Strain (mm/mm)	Stress (MPa)	Strain (mm/mm)
0.000083	291.98	0.0914	301.69	0.106	281.05	0.0838	199.43	0.0689
0.00083	302.33	0.1155	307.21	0.1195	314.42	0.098	220.01	0.0773
0.0083	323.72	0.1273	313.77	0.1277	321.76	0.1273	238.66	0.0856

**Table 6** The maximum compression stress ( $C_2$ ) and strain values corresponding to this stress in weft direction

Strain rates ( $/s^{-1}$ )	− 20 °C		0 °C		20 °C		80 °C	
	Stress (MPa)	Strain (mm/mm)	Stress (MPa)	Strain (mm/mm)	Stress (MPa)	Strain (mm/mm)	Stress (MPa)	Strain (mm/mm)
0.000083	294.73	0.1383	314.16	0.1189	264.44	0.0914	227.95	0.1023
0.00083	381.28	0.1439	334.25	0.1331	326.80	0.1199	267.18	0.1105
0.0083	401.21	0.1523	357.37	0.1773	357.73	0.1339	290.42	0.1439

**Table 7** The absorbed energy of S glass/epoxy composites under tensile loading

Strain rates ( $/s^{-1}$ )	Weft direction ( $MJ/m^3$ )				Wrap direction ( $MJ/m^3$ )			
	− 20 °C	0 °C	20 °C	80 °C	− 20 °C	0 °C	20 °C	80 °C
0.000083	2.328	3.151	3.157	2.374	2.714	5.589	4.846	3.230
0.00083	3.070	3.689	4.120	2.792	7.114	7.273	5.504	4.182
0.0083	1.114	3.747	4.152	3.664	6.221	8.110	7.029	5.622

**Table 8** The fracture energy of S glass/epoxy composites under compression loading

Strain rates ( $/s^{-1}$ )	Weft direction ( $MJ/m^3$ )				Wrap direction ( $MJ/m^3$ )			
	− 20 °C	0 °C	20 °C	80 °C	− 20 °C	0 °C	20 °C	80 °C
0.000083	22.419	20.663	14.773	12.784	13.521	16.932	12.607	6.752
0.00083	31.031	26.651	21.240	17.492	19.978	18.687	17.307	9.225
0.0083	28.932	29.558	22.632	16.207	17.693	22.092	20.028	7.153

8 according to woven directions. The behavior of the stress–strain curve, until the test sample is completely damaged (until fracture point), can be used to determine the absorbed energy. The Riemann Addition Method is used to determine the amount of energy absorbed, which is equal to the area under the stress–strain curve.[20, 35]. When looking at Tables 5 and 6, it can be seen that the strain rate and the ambient temperature do not have a linear effect on the absorbed energy. Such that, if the temperature increases from − 20 to 80 °C for the same deformation rate, the absorbed energy value reaches its maximum value at 20 °C and while temperature increases to 80 °C from that point, it tends to fall down. On the other hand, when the strain rate increases for the same temperature value, the absorbed energy value increases. But this phenomenon did not occur at − 20 °C degrees. Increasing strain rate causes crisp of S glass/epoxy composite material. The composite material also exhibited brittle deformation behavior at cold temperatures. The

overlap of these two embrittlement effects creates a negative effect on the energy to be absorbed by the material.

The failure mode under tensile loading is in the form of matrix and fiber breakage, while the major failure modes for the unidirectional laminated composite under compression load are delamination, splitting and crushing. During the formation of the failure modes that occur during the compression loading, the S2 glass/epoxy composite material was more deformed than the tensile loading. Compared to the tensile loading, S2 glass/epoxy laminated composites has suffered damage at lower stress values under compression loading. On the other hand, composite test samples had more deformation amount under compression loading. This is the reason why S2 glass/epoxy laminated composites have more fracture damage energy under compression load than tensile loading.

## 3.2 Dynamic mechanical analysis

In the dynamic mechanical analysis (DMA) study, viscoelastic behavior of S2 glass/epoxy composite plates was investigated in terms of storage modulus ( $E'$ ), loss modulus ( $E''$ ) and  $\tan \delta$  depending on the fiber orientation. Test specimens with warp, weft and diagonal ( $45^\circ$  angle fiber direction) directions were tested. The homogeneous or heterogeneous nature of different fiber directions was also investigated using Cole–Cole plots.

### 3.2.1 Storage modulus ( $E'$ )

Storage modulus ( $E'$ ) is a measure of elastic response which is defined as the maximum energy stored by polymer-based fibrous composites during one cycle of loading. The variation in storage modulus of S2 glass/epoxy as a function of temperature at 1 Hz frequency is shown in Fig. 9. There are three significant regions (glassy, transition and rubbery) that can be seen in Fig. 9. The relatively flat regions at the lower temperatures correspond to the glassy (rigid) state of each polymer. In the glassy region, it is observed that S2 glass/epoxy composites have a higher value of  $E'$  due to showing brittle behavior which is a further cause of uniform transfer of stress. The highest storage modulus in the warp direction was obtained as 18.36 GPa at a temperature of  $-28.54^\circ\text{C}$ . Similarly, the maximum storage modulus in the weft direction is 16.35 GPa observed at  $-27.15^\circ\text{C}$ . On the other hand, the maximum storage modulus was observed as 11.48 GPa at  $-29.93^\circ\text{C}$  for the specimen having  $45^\circ$  fiber orientation.

One important application of DMA is the measurement of the glass transition temperature of polymers. In the transition region, it was seen that S2 glass/epoxy composites have a gradual fall in values of  $E'$  with an increase in temperature; whereas, epoxy resin has a sudden fall because of an increase in molecular mobility as the temperature reached above to  $T_g$ . The polymer glass transition ( $T_g$ ) starts where the curves initially bend downward. In this elastic region, the resin matrix loses its cohesive bond strength. In terms of all three fiber orientations, there is a rapid drop in storage modulus, especially from a temperature of  $88^\circ\text{C}$ . In the transition region, although the modulus values  $E'$  of the samples in the warp and weft directions are close to each other, the modulus value  $E'$  in the diagonal direction is approximately one-third of them. In the rubbery region, higher temperature accelerates the materials mobility and  $E'$  of S2 glass/epoxy exhibits horizontal behavior despite temperature increase for each fiber direction. With the temperature increase for all three test types of specimens, storage modulus, which are the usual result of DMA tests, tend to fall.

### 3.2.2 Loss modulus ( $E''$ )

Loss modulus ( $E''$ ) is a measure of viscous response of composite material and it measures the energy dissipated as heat. Figure 10 shows the loss modulus of the S2 glass/epoxy-laminated composite material. Although the loss modulus values for different fiber orientations have different peaks, they exhibited similar behavior with respect to temperature increase. The loss modulus of S2 glass/epoxy composite material in warp, weft, and diagonal direction are close to

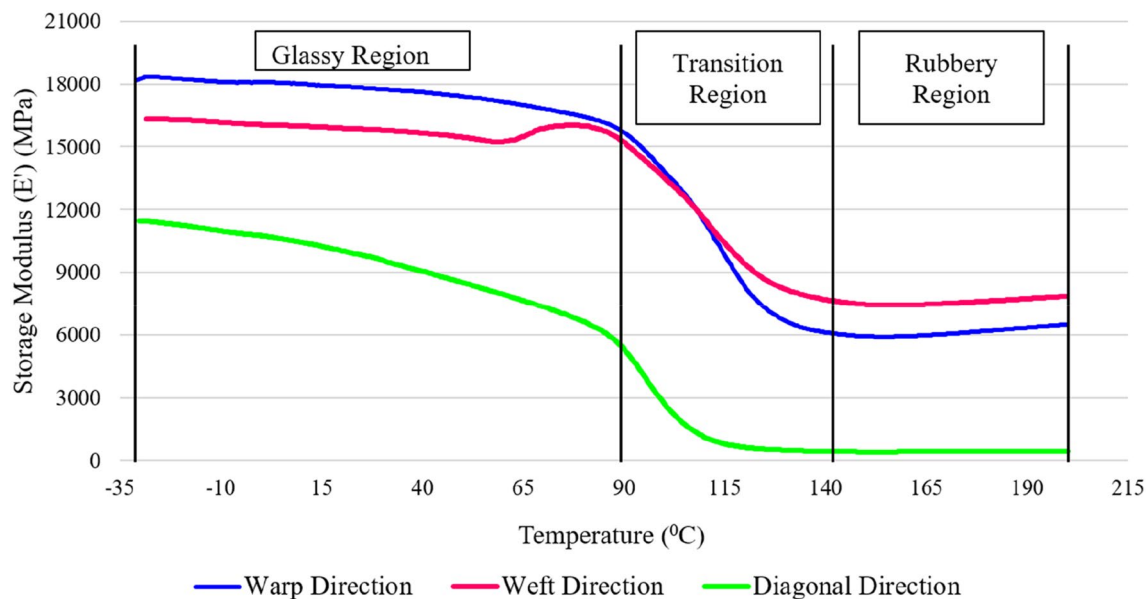
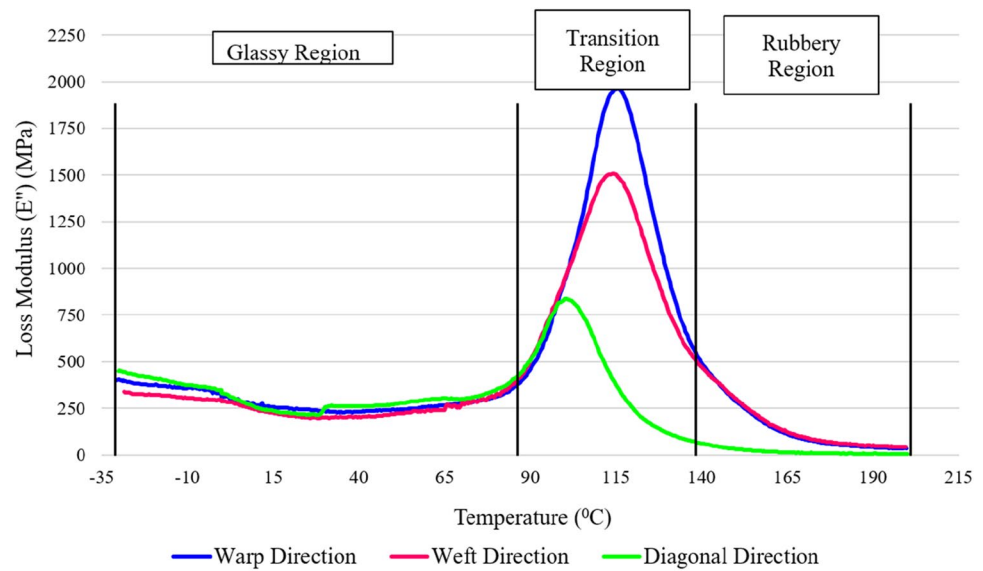


Fig. 9 Elastic response of S2 glass/epoxy according to fiber orientation

**Fig. 10** The viscous response of S2 glass/epoxy according to fiber orientation



each other in the glassy region. The temperature increase through the transition region did not cause a change in the loss modulus of the composite material. By the increasing temperature in the transition region, the loss module value first increased and then decreased. Between 100 and 116 °C, the loss modulus value has reached its maximum value for all fiber directions. In the warp direction test specimens, the highest loss modulus was found to be 1964.53 MPa where the temperature was 115.55 °C, while the highest loss modulus of the weft direction test specimens was found to be 1509.79 MPa at 114.01 °C. The highest loss modulus at 45° fiber direction test specimens was 835.47 MPa at 100.62 °C. The maximum increase in loss modulus by the increase of temperature was seen in the sample with fiber orientation in the wrap direction. The least amount of increase was observed at samples with fiber orientation in the diagonal direction. Similar to storage modulus, curves for the rubbery region, all the curves were overlapping with each other which indicates that at higher temperatures, there is no significant change in  $E''$ .

The storage and loss modulus are the results of the interface bond between the fiber and the epoxy. The higher the storage and loss modulus, the better the interface bond [25]. While the epoxy/fiber interface bond has the highest warp direction orientation, the 45° angle of fiber orientation is the weakest. While the fiber/epoxy interface bond has the highest warp direction orientation, diagonal fiber orientation is the weakest.

### 3.2.3 Damping factor ( $\text{Tan}\delta$ )

Damping factor ( $\text{Tan}\delta$ ) is the ratio of loss to the storage and is called damping. It is a measure of the energy dissipation of material. It tells us how good material will be at

absorbing energy. The  $\text{Tan}\delta$  modulus value can be said to be related to the impact strength of the composite material. The discontinuous phase of reinforcement in composite materials makes a big contribution to its damping behavior. The lower  $\text{Tan}\delta$  value in the damping graph indicates that there is good interfacial adhesion between fiber and matrix material [36, 37]. Figure 11 shows the damping behavior of S2 glass/epoxy composites as a function of temperature at a frequency rate of 1 Hz according to three different fiber directions. From Fig. 11, it is clear that the S2 glass/epoxy composites have shown the lower  $\text{Tan}\delta$  value which is attributed to the higher load-carrying capacity of wrap direction. The best behavior in force damping with temperature increase is shown by test specimens in the wrap direction, while the specimens with diagonal fiber direction were the weakest in temperature-dependent force damping.

If the glass transition temperature of the S2 glass/epoxy composite material is desired to be determined using the storage module-temperature graph, tangents should be drawn to the curves in the glassy and transition region. The intersection point of the plotted tangents gives the glass transition temperature of the composite material [33]. On the other hand, glass transition temperature ( $T_g$ ) of the polymeric composites is the peak point of either  $E''$  or  $\text{Tan}\delta$  curve [38]. Table 9 shows the transition temperature values obtained from storage modulus, loss modulus, and  $\text{Tan}\delta$  curves. Transition temperatures obtained from loss modulus and  $\text{Tan}\delta$  curves were found to be relatively close to each other. In addition, the glass transition temperature values obtained from the storage module is lower than the transition temperature values obtained from other graphs. Haque et al. [39] obtained glassy transition temperatures between 128 and 134.11 °C with silica nanoparticles and S2 glass. With the effect of the resin and hardener used, obtaining a glass

**Fig. 11** Variation in  $\text{Tan } \delta$  with the temperature of S2 glass/epoxy according to fiber orientation

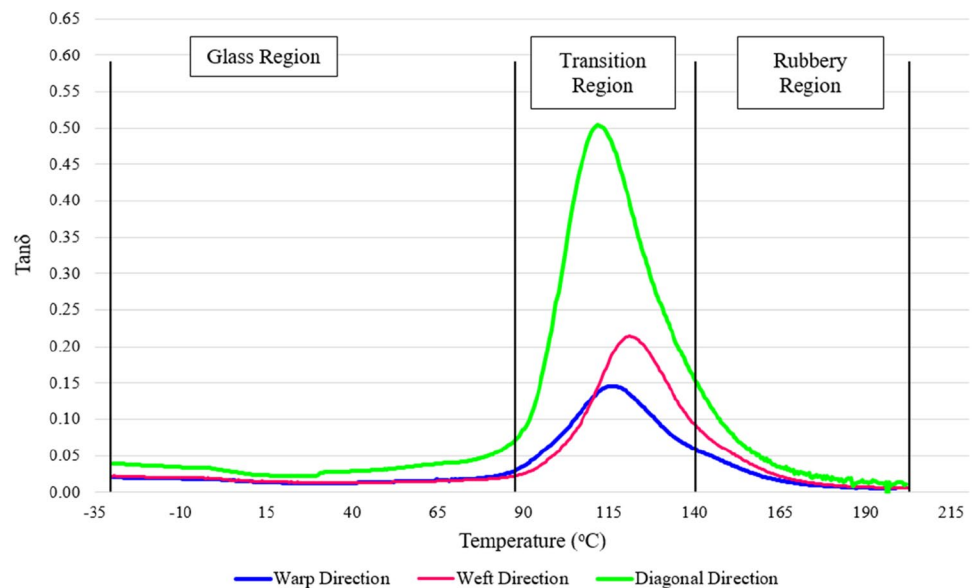


**Table 9** Glass transition temperature from storage modulus, loss modulus, and damping curve

	$T_g$ for $E'$ (°C)	$T_g$ for $E''$ (°C)	$T_g$ for $\text{Tan } \delta$ (°C)	Peak of $\text{Tan } \delta$
Wrap direction	94.88	115.50	116.13	0.1460
Weft direction	94.11	114.01	121.05	0.2143
Diagonal direction	88.91	100.63	112.27	0.5035

transition temperature between the two studies examined also showed compatibility with the literature.

### 3.2.4 Cole–Cole plot

In the literature, the Cole–Cole method is used to show the changes in the viscoelastic properties of the material. The Cole–Cole equation is a relaxation model that is often used to describe dielectric relaxation in polymers materials. In addition, it can be used to understand the structural changes occurred in the cross-linked polymers after incorporating reinforcement with polymeric matrices. Figure 12 shows the Cole–Cole plots of S2 glass/epoxy composites, whereas the loss modulus was plotted as a function of storage modulus. A perfect semicircular-shaped curve on Cole–Cole plots is an indication of a homogeneous polymeric system [40]. According to the curves obtained from the samples tested in the Wrap and Weft direction, it can be said that the test samples are relatively homogeneous. In this study, we obtained imperfect circles indicative of the heterogeneity of the system. The slope in the sample tested in the diagonal direction shows a horizontal behavior after 7000 MPa storage module. However, the shape of the curve shows a relatively good fiber/matrix adhesion.

### 3.3 TGA analysis

TGA tests were carried out with the test specimens taken from the first and last plates of the manufactured composite plates. During the test, the temperature was increased from 25 to 600 °C. When the TG-temperature graph in Fig. 13 is examined, very stable mass conservation is observed up to 272 °C, and the decomposition has started since this temperature. When the temperature reached 530 °C, the decomposition stopped weight started to remain constant. 530 °C temperature point represented the final char yield. From this temperature, it is understood that pure fiber remains in the test ambience.

The DTG curves are more convincing to study the degradation process. There were three main degradation regions ranging from 300 to 312 °C, 312 to 337 °C, and 337 to 530 °C. In these temperature ranges, the resin/hardener pair started to boil. Gas bubbles formed during boiling momentarily caused weight increase or decrease.

## 4 Conclusions

In this study, the static and dynamic behavior of S2 glass fiber-reinforced laminated composite structures, which are widely used in the aviation industry, at different temperatures



**Fig. 12** Effect of dynamic loading on Cole–Cole plots of S2 glass/epoxy composites

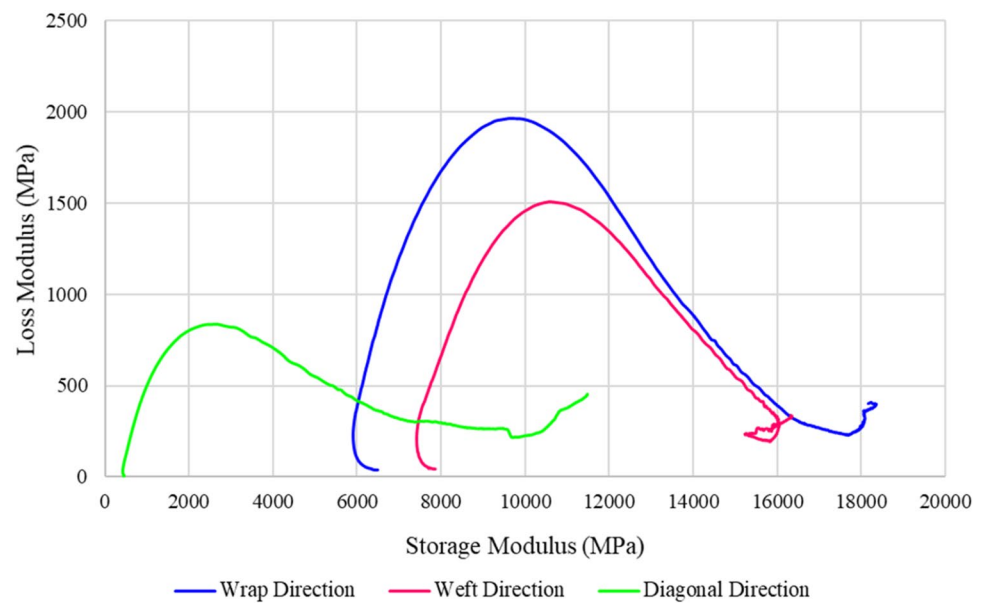
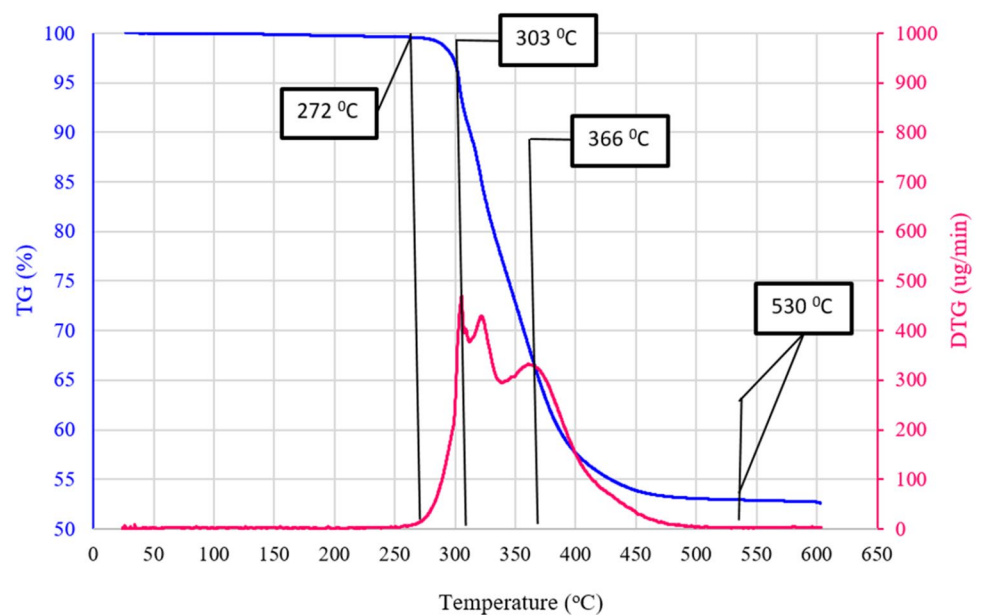


**Fig. 13** TGA analysis of S2 glass/epoxy-laminated composite



and different strain rates were characterized. In addition, TGA analysis was performed to better define the relationship between resin/hardener set and S glass fiber fabric. From the results, the following conclusions can be drawn;

- It can be said according to the static test result, the maximum stress, and maximum strain increase with increasing strain rate for all temperatures and for each loading type. However, there is not always a linear relationship between the absorbed energy and the strain rate. While there is a linear relationship for 0 °C and 20 °C, the absorbed energy value decreases at a high strain rate (0.0083) at – 20 °C and 80 °C. It can be said that this is

caused by the sudden embrittlement effect caused by the high temperature and high strain rate in the structure of the material. The damaged area which gives 2D information on the extent of damage was measured by visual inspection. The visual inspection of the failed specimens shows significant changes in the fracture surface with an increased strain rate. Increasing the strain rate leads to the development of different mechanical relationships between the fiber and the matrix so that different failure modes occur in the composite plate.

- All types of damage that may occur in laminated composite plates were observed during static and dynamic tests. Damage types such as delamination, matrix

fracture, and fiber rupture are the most common. In addition, micro-cracks were observed around the damage zone. For thermoset resins (epoxy), the higher the energy input, the faster and the longer the cracks propagate. At low tensile rates, the damage takes up a small area on the sample since the deformation occurs slowly and the stress distribution is homogeneously distributed. As the strain rate increased, the deformation occurred rapidly and the stresses could not be distributed homogeneously on the sample. Thus, due to the high-stress concentration in the damage zone, the damage zone extends over a larger area.

- The tensile and compressive strength increased approximately linearly with the values of strain rate, and a time-temperature model could be fitted to the data over a wide range of strain rates.
- When the modulus of elasticity values obtained from static tests and storage modulus values obtained from dynamic tests are compared, it has been observed that they show similar behavior in the glassy region ( $-20\text{ }^{\circ}\text{C}$  and  $80\text{ }^{\circ}\text{C}$ ). According to the static and dynamic test results, the decrease in elasticity modulus value with increasing temperature is more prominent for weft weaving direction. For the dynamic loading condition, S2 glass/epoxy composite plate is positioned in the warp direction, it is seen that it is more resistant to loading conditions under repeated and variable temperatures than other types of orientation.

**Acknowledgements** This study was supported by Usak University Scientific Research Agency. Project number: 2018/MF003 scientific research project.

## References

1. A. Acharya, *Metal Oxide Glass Fibers* (Elsevier, Amsterdam, 2020). <https://doi.org/10.1016/B978-0-12-817458-6.00016-0>
2. A. Karmakar, A. Ghosh, Dielectric permittivity and electric modulus of polyethylene oxide (PEO)-LiClO<sub>4</sub> composite electrolytes. *Curr. Appl. Phys.* **12**, 539–543 (2012). <https://doi.org/10.1016/j.cap.2011.08.017>
3. S. Bhattacharya, R. Kundu, K. Bhattacharya, A. Poddar, D. Roy, Micromechanical hardness study and the effect of reverse indentation size on heat-treated silver doped zinc-molybdate glass nanocomposites. *J. Alloys Compd.* **770**, 136–142 (2018). <https://doi.org/10.1016/j.jallcom.2018.08.085>
4. R. Kundu, D. Roy, S. Bhattacharya, Microstructure, electrical conductivity and modulus spectra of CdI<sub>2</sub> doped nanocomposite-electrolytes. *Phys. B Phys. Condens. Matter* **507**, 107–113 (2016). <https://doi.org/10.1016/j.physb.2016.11.036>
5. S.M. Mullaikodi, K. Shanmugasundaram, V.S. Rao, S. Rangarajan, Synthesis, characterization and machinability studies on thin hybrid composites with SiC nano particles. *Mater. Res. Express* (2019). <https://doi.org/10.1016/j.jhazmat.2007.01.073>
6. M. Alsaadi, A. Erklig, A comparative study on mode I and mode II interlaminar behavior of borax and SiC particles toughened S-glass fabric/epoxy composite. *Arab. J. Sci. Eng.* **42**, 4759–4769 (2017). <https://doi.org/10.1007/s13369-017-2649-1>
7. M. Bulut, A. Erklig, E. Yeter, Hybridization effects on quasi-static penetration resistance in fiber reinforced hybrid composite laminates. *Compos. Part B Eng.* **98**, 9–22 (2016). <https://doi.org/10.1016/j.compositesb.2016.05.025>
8. T. Archana, S. Anand Kumar, R.R. Elangovan, Y.S. Rammohan, R. Dumpala, B. Ratna Sunil et al., Fracture toughness and fatigue behavior of spider silk and S-glass epoxy composites: an FEM approach. *Mater. Today Proc.* **5**, 2627–2634 (2018). <https://doi.org/10.1016/j.matpr.2018.01.042>
9. J. Reiner, J.P. Torres, M. Veidt, A novel top surface analysis method for mode I interface characterisation using digital image correlation. *Eng. Fract. Mech.* **173**, 107–117 (2017). <https://doi.org/10.1016/j.engfracmech.2016.12.022>
10. Fotouhi M, Jalalvand M, Prato A, Wisnom MR, Thin ply carbon/glass hybrid laminates to activate new damage mechanisms under indentation. In Proceedings of the 18th European Conference Composites Materials-ECCM18 (2018), pp. 24–8
11. Z. Liu, P. Li, N. Srikanth, T. Liu, G.B. Chai, Quantification of flexural fatigue life and 3D damage in carbon fibre reinforced polymer laminates. *Compos. Part A Appl. Sci. Manuf.* **90**, 778–785 (2016). <https://doi.org/10.1016/j.compositesa.2016.09.008>
12. A. Moudood, A. Rahman, H.M. Khanlou, W. Hall, A. Öchsner, G. Francucci, Environmental effects on the durability and the mechanical performance of flax fiber/bio-epoxy composites. *Compos. Part B Eng.* **171**, 284–293 (2019). <https://doi.org/10.1016/j.compositesb.2019.05.032>
13. K. Yang, S. Wu, J. Guan, Z. Shao, R.O. Ritchie, Enhancing the mechanical toughness of epoxy-resin composites using natural silk reinforcements. *Sci. Rep.* **7**, 1–9 (2017). <https://doi.org/10.1038/s41598-017-11919-1>
14. B. Hulugappa, M.V. Achutha, B. Suresha, Effect of environmental conditions on flexural strength and fracture toughness of particulate filled glass-epoxy hybrid composites. *Mater. Sci. Appl.* **07**, 710–729 (2016). <https://doi.org/10.4236/msa.2016.711057>
15. D. Scida, M. Assarar, C. Poilâne, R. Ayad, Influence of hygro-thermal ageing on the damage mechanisms of flax-fibre reinforced epoxy composite. *Compos. Part B Eng.* **48**, 51–58 (2013). <https://doi.org/10.1016/j.compositesb.2012.12.010>
16. V.P. Nikolaev, E.V. Myshenkova, V.S. Pichugin, E.N. Sinitsyn, A.N. Khoroshev, Temperature effect on the mechanical properties of composite materials. *Inorg. Mater.* **50**, 1511–1513 (2014). <https://doi.org/10.1134/s002016851415014x>
17. G. Aklilu, S. Adali, G. Bright, Temperature effect on mechanical properties of carbon, glass and hybrid polymer composite specimens. *Int. J. Eng. Res. Afr.* **39**, 119–138 (2018). <https://doi.org/10.4028/www.scientific.net/jera.39.119>
18. L. Cadieu, J.B. Kopp, J. Jumel, J. Bega, C. Froustey, Strain rate effect on the mechanical properties of a glass fibre reinforced acrylic matrix laminate. An experimental approach. *Compos. Struct.* **223**, 110952 (2019). <https://doi.org/10.1016/j.compositestruct.2019.110952>
19. G.H. Staab, A. Gilat, High strain rate response of angle-ply glass/epoxy laminates. *J. Compos. Mater.* **29**, 1308–1320 (1995). <https://doi.org/10.1177/002199839502901003>
20. M. Aktas, H.E. Balcioglu, G. Kùlahli, Strain rate effects on tensile and compressive behaviour of woven-knitting glass/epoxy composites. *Adv. Compos. Lett.* **22**, 13 (2013)
21. C. Chen, C. Zhang, C. Liu, Y. Miao, S.C. Wong, Y. Li, Rate-dependent tensile failure behavior of short fiber reinforced PEEK. *Compos. Part B Eng.* **136**, 187–196 (2018). <https://doi.org/10.1016/j.compositesb.2017.10.031>

22. O.I. Okoli, G.F. Smith, The effect of strain rate and fibre content on the Poisson's ratio of glass/epoxy composites. *Compos. Struct.* **48**, 157–161 (2000)
23. F. Fereshteh-Saniee, G.H. Majzoobi, M. Bahrami, An experimental study on the behavior of glass-epoxy composite at low strain rates. *J. Mater. Process Technol.* **162**, 39–45 (2005). <https://doi.org/10.1016/j.jmatprotec.2005.02.011>
24. Dunson D, Characterization of polymers using dynamic mechanical analysis (DMA). EAG Appl Note (2017)
25. A. Vasudevan, S. Senthil Kumaran, K. Naresh, R. Velmurugan, Experimental and analytical investigation of thermo-mechanical responses of pure epoxy and carbon/Kevlar/S-glass/E-glass/epoxy interply hybrid laminated composites for aerospace applications. *Int. J. Polym. Anal. Charact.* **23**, 591–605 (2018). <https://doi.org/10.1080/1023666X.2018.1468599>
26. A. Haque, M. Shamsuzzoha, F. Hussain, D. Dean, S2-glass/epoxy polymer nanocomposites: manufacturing, structures, thermal and mechanical properties. *J. Compos. Mater.* **37**, 1821–1838 (2003). <https://doi.org/10.1177/002199803035186>
27. R. Rangaraj, J. Prabhakaran, S. Gopal, K. Kannan, P. Ramesh, Dynamic mechanical properties and glass transition temperature analysis of Kevlar/glass fiber epoxy hybrid composites. *GRD J. Eng.* **2**, 12–16 (2017)
28. AZO Materials, S-Glass Fibre 2001:1–3. <https://www.azom.com/properties.aspx?ArticleID=769>. Accessed 23 July 2019.
29. HEXION® Specialty Chemicals. Laminating Resin MGS® L 285 Hardeners MGS® 285-287 Technical Data Sheet n.d. <https://www.hexion.com/en-US/search?id=30303>. Accessed 23 July 2019
30. ASTM International, *Designation: D 3039/D 3039M–00 Standard Test Method for Tensile Properties of Polymer Matrix Composite Materials* (ASTM International, West Conshohocken, 3039M), pp. 1–15. [https://doi.org/10.1520/D3039\\_D3039M-08](https://doi.org/10.1520/D3039_D3039M-08)
31. S. Sugiman, M.H. Gozali, P.D. Setyawan, Hygrothermal effects of glass fiber reinforced unsaturated polyester resin composites aged in steady and fluctuating conditions. *Adv. Compos. Mater.* **3046**, 1–16 (2017). <https://doi.org/10.1080/09243046.2017.1405597>
32. ASTM International, ASTM-D3410 standard test method for compressive properties of polymer matrix composite materials with unsupported gage section by shear loading. *Annu. B ASTM Stand.* **15**(03), 1–16 (2003). <https://doi.org/10.1520/D3410>
33. ASTM, Standard test method for glass transition temperature (DMA Tg) of polymer matrix composites by dynamic mechanical analysis (DMA). ASTM Int. (2007). <https://doi.org/10.1520/D7028-07E01.2>
34. ASTM E1131, Standard test method for compositional analysis by thermogravimetry. *Annu B ASTM Stand* (2003), pp. 1–5
35. M.M. Shokrieh, M.J. Omid, Tension behavior of unidirectional glass/epoxy composites under different strain rates. *Compos. Struct.* **88**, 595–601 (2009). <https://doi.org/10.1016/j.compstruct.2008.06.012>
36. A. Atiqah, M. Jawaid, S.M. Sapuan, M.R. Ishak, Dynamic mechanical properties of sugar palm/glass fiber reinforced thermoplastic polyurethane hybrid composites. *Polym. Compos.* **40**, 1329–1334 (2019). <https://doi.org/10.1002/pc.24860>
37. M. Jawaid, H.P.S. Abdul Khalil, A. Hassan, R. Dungani, A. Hadiyane, Effect of jute fibre loading on tensile and dynamic mechanical properties of oil palm epoxy composites. *Compos. Part B Eng.* **45**, 619–624 (2013). <https://doi.org/10.1016/j.compositesb.2012.04.068>
38. J. Naveen, M. Jawaid, E.S. Zainudin, M.T.H. Sultan, R. Yahaya, M.S. Abdul Majid, Thermal degradation and viscoelastic properties of Kevlar/*Cocos nucifera* sheath reinforced epoxy hybrid composites. *Compos. Struct.* **219**, 194–202 (2019). <https://doi.org/10.1016/j.compstruct.2019.03.079>
39. A. Haque, F. Hossain, D. Dean, M. Shamsuzzoha, S2-glass/vinyl ester polymer nanocomposite S2-glass/vinyl ester polymer nanocomposites: manufacturing, structures, thermal and mechanical properties. *J. Compos. Mater.* **37**, 1821–1837 (2003)
40. L.U. Devi, S.S. Bhagawan, S. Thomas, Dynamic mechanical analysis of pineapple leaf/glass hybrid fiber reinforced polyester composites. *Polym. Compos.* **31**, 956–965 (2010). <https://doi.org/10.1002/pc.20880>

**Publisher's Note** Springer Nature remains neutral with regard to jurisdictional claims in published maps and institutional affiliations.